

From mach cone to reappeared jet: What do we learn from PHENIX results on non-identified jet correlation?

Jiangyong Jia for the PHENIX Collaboration

Columbia University, New York, NY 10027 and Nevis Laboratories, Irvington, NY 10533, USA

Abstract. High p_T jets are known to be strongly modified by the dense, strongly interacting medium created in heavy-ion collisions. The jet signal, extracted from two particle $\Delta\phi$ correlation, shows a systematic evolution of these modifications as function of p_T and centrality. At intermediate p_T , both near side and away side correlations are modified. But the modifications are much stronger at the away side, resulting in a characteristic cone type of structure in central Au + Au collisions. The robustness of cone structure is strengthened by studying the jet shape as function of angle relative to the reaction plane. As one increase the p_T for BOTH hadrons, the cone structure seems to be filled up, and a peak structure appears on the away side. However, the interpretation of these results require careful separation of medium effect and surface bias.

PACS: 27.75.-q

INTRODUCTION

High p_T back-to-back jets from hard-scattering were shown to be a valuable probe for the sQGP [1] created in heavy-ion collisions at RHIC. Existing two particle jet correlation results from RUN2 statistically limited Au + Au data set at RHIC have revealed a strong and complicated modification of the jets by the medium. On the one hand, jet correlation at high p_T indicates a seemingly complete disappearance of the away side jet signal [2]. On the other hand, as one lower the threshold on the second particle, one find that the away side jet yield is significantly enhanced [3] but broadened [4]. Qualitatively, this is consistent with the energy loss picture, where the high p_T jet are quenched by the medium and their lost energy become redistributed in the soft region.

Equipped with excellent statistics from RUN4 Au + Au and RUN5 Cu + Cu data sets, we would like to gain further understanding on the interaction of the jets with the medium. We hope to address important questions such as: How the jet loses its energy? How the lost energy get redistributed? How the medium responds to the jet? What happens to the higher p_T jets? We attempt to address these questions using the non-identified charged hadron - charged hadron correlation results from RUN4 Au + Au data set.

JET PROPERTIES AT INTERMEDIATE P_T

Our analysis are based on 1 billion minimum bias events from Au + Au collisions at $\sqrt{s} = 200$ GeV, about two third of the full data set. The correlation function $C(\Delta\phi)$ (CF) is

constructed as the ratio of same event pair distribution, $dN^{\text{pairs}}/d\Delta\phi$ to the mixed event pair distribution, $dN^{\text{mix}}/d\Delta\phi$. $dN^{\text{mix}}/d\Delta\phi$ reflects the level of combinatoric background pair and properly simulates the geometrical pair acceptance [5], but does not include any real correlations which appear only in the same event pair distribution. In heavy-ion collisions, such real correlations come mainly from jets and elliptic flow, and the CF can be expressed as,

$$C(\Delta\phi) = J(\Delta\phi) + \xi (1 + 2v_2^t v_2^a \cos 2\Delta\phi) \quad (1)$$

The superscript t and a stand for the trigger and associated particles, ξ is a normalization factor which is the ratio of the combinatorics pairs in the same event to those in the mixed event. ξ is typically bigger but very close to 1.

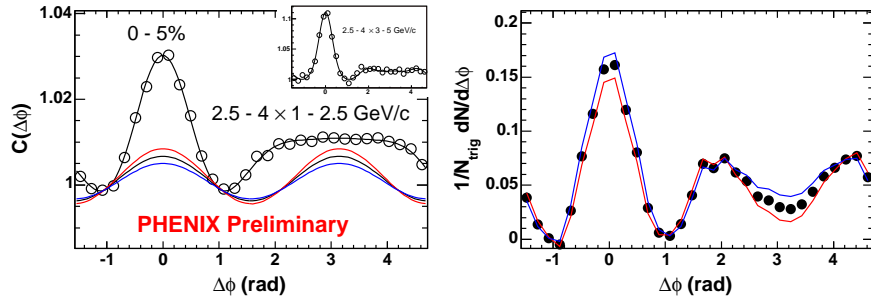


FIGURE 1. a) Correlation function in 0-5% centrality bin, the lines indicated the level of flow background and it's systematic error band, the insert is CF for higher $p_{T,\text{assoc}}$. b) Correspondingly background subtracted per-trigger yield.

Fig.1a shows the typical correlation function from central Au + Au collisions. The away side shapes are very broad but highly non-gauss like. It has a wide plateau that expands about 2 radian and a possible small dip at π . The subtraction of the flow contribution (shown by the curves) can only make the dip even deeper, as shown in Fig1b. ξ is fixed by scaling the flow term to match the $C(\Delta\phi)$, which is equivalent to assuming $J = 0$ at some $\Delta\phi$ (ZYAM) [6]. The ZYAM procedure results in an over-subtraction of jet yield, however since $2v_2^t v_2^a \approx \text{few \%}$, the over-subtraction (a couple percent change in ξ) mainly results in a vertical shift and does not affect the away side jet shape. The systematic error on $J(\Delta\phi)$ is more sensitive to the uncertainties of v_2 themselves.

PHENIX has done a systematic study of the jet shape and yield at intermediate p_T , as shown in Fig.2. There is a continues evolution of the split and the dip as function of centrality and p_T . The away side split is characterized by the split parameter D [7], which is obtained by a double gauss fit on the away side. D seems to turn on rather quickly as a function of centrality, and fall on a uniform curve as function of N_{part} for different collision energies and collision systems.

What is the nature of the away side split? The standard broadening of the jets due to energy loss can not produce the dip or the flat jet structure at the away side due to it's random walk nature [8]. Models with cherenkov [9, 10] or medium dragging effect [11] can produce a significant broadening jet structure on the away side, but the cone angle has a strong momentum dependence and is expected to disappear quickly at large p_T . On the other hand, Casalderrey *et. al.* [12] has proposed a “mach cone”/“shock

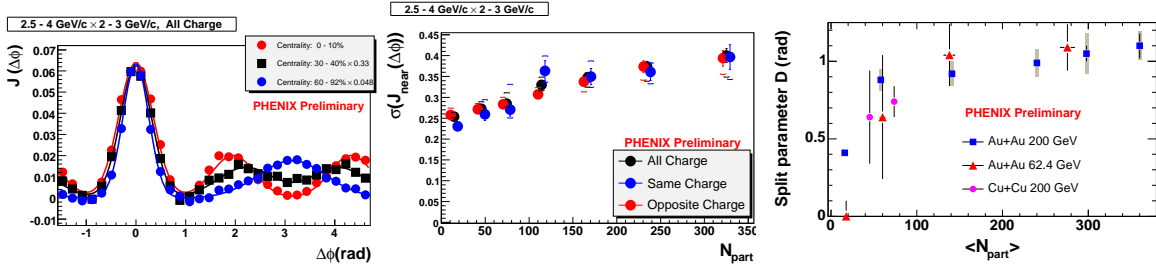


FIGURE 2. a) The correlation function for central, mid-central and peripheral bin, b), the near side width as function of centrality for same charged pairs, opposite charged pairs and all pairs, c) The away side “D” parameter as function of N_{part} .

wave” mechanism which can produce a dip structure on the away side. The shock wave happens because the jet travels faster than sound in the medium, resulting in a collective excitation of the medium at a fixed angle $\theta = \cos^{-1}(c_s/c)$, where c_s is the speed of sound of the medium. The direction of the cone is expected to be independent of the associated p_T , but the width of the cone narrows with increasing p_T .

In contrast to the strong modification of the away side jet shape, Fig.2 also indicate a sizable broadening of the near side jet width in central collisions. This could be a natural consequence of the strong interaction of jets with the medium. Due to the surface emission bias [14], the average distance travelled by the near side jet is much smaller than that for the away side jet. But the relatively small amount of medium that the near side jet has to go through might already lead to some broadening. On the other hand, we know that the baryon yield is enhanced at intermediate p_T [15]. Since the near side jet structure could be different between baryon trigger and meson trigger [16], the broadening of the near side jet width could be a consequence of the very different particle composition between central and peripheral collisions.

To quantify the modification of the away side jet, we extract the jet yield in three different $\Delta\phi$ regions: near side jet region ($|\Delta\phi| < \pi/3$), the away side dip region ($|\Delta\phi - \pi| < \pi/6$), and the away side shoulder region ($|\Delta\phi - \pi \pm \pi/3| < \pi/6$). The shoulder region is sensitive to the novel medium effects such as shock wave or cerenkov gluons, while the dip region is sensitive to the fraction of punch through jet. Fig.3 plots the jet yield for the three regions as function of p_T for various centralities. We notice that there is large separation between the yields for the dip region and near side jet region in most central bin persistent to large p_T . While in peripheral bins, the two are close to each other. Also in peripheral bins, the yield from the dip region exceeds that from the shoulder region. This reflects the normal narrowing of the away side jets for higher p_T .

DEPENDENCE ON THE REACTION PLANE.

The study of the jet yield as function of angle w.r.p to reaction plane is very important in the sense that it adds another dimension in controlling the path length dependence. As we demonstrate in this section, it also provide additional constrains on the subtraction of the elliptic flow.

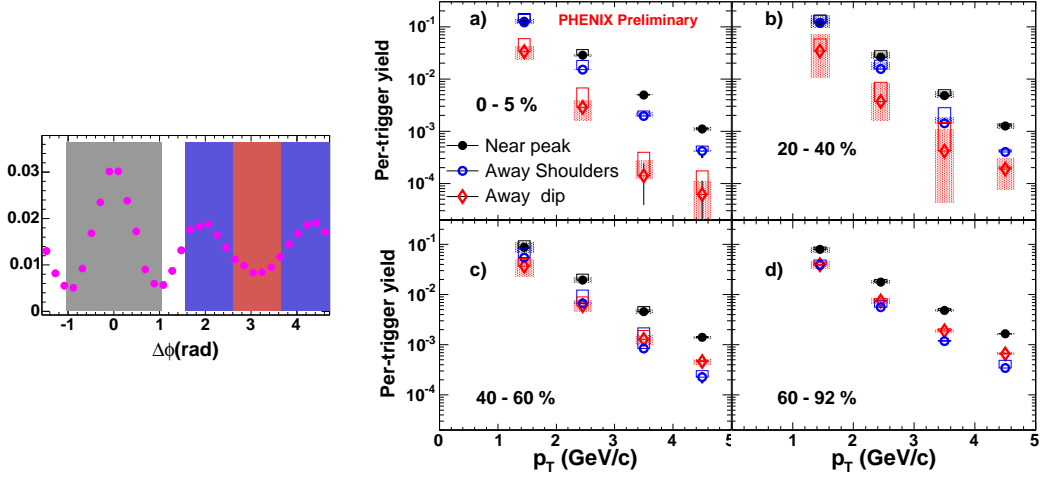


FIGURE 3. Three integration ranges (left) The yield for trigger 2.5-4 GeV/c plotted as function of associated hadron p_T for four different centrality bins (right).

When the trigger particles are selected in a window centered around ϕ_s with a width of $\pm c$ respect to the reaction plane, the pair distribution up to second order harmonics is [13]:

$$\frac{dN^{\text{pairs}}}{d\Delta\phi} = \frac{2c}{\pi} B(a + 2v_2^a b \cos 2\Delta\phi)$$

$$\begin{cases} a = 1 + 2v_2^t \cos 2\phi_s \frac{\sin 2c}{2c} \langle \cos 2\Psi \rangle \\ b = v_2^t + \cos 2\phi_s \frac{\sin 2c}{2c} \langle \cos 2\Psi \rangle + v_2^t \cos 4\phi_s \frac{\sin 4c}{4c} \langle \cos 4\Psi \rangle \end{cases}$$

a is the combinatoric background level, which is proportional to the number of triggers in the window. Thus the correlation function goes like

$$C(\Delta\phi) = \frac{dN^{\text{pairs}}/d\Delta\phi}{dN^{\text{mix}}/d\Delta\phi} = \xi(1 + 2v_2^a b/a \cos 2\Delta\phi) = \xi(1 + 2v_2^t v_{2,\text{eff}}^t \cos 2\Delta\phi) \quad (2)$$

Where $v_{2,\text{eff}}^t = b/a$ is the effective v_2 of the trigger particle in the window, and ξ is the same normalization factor which appears in Eq.1. ξ does not depends on the trigger direction.

In this analysis, we divide the trigger direction ($[0, \pi/2]$) into 6 different trigger bins. According to Eq.2, we have six different equations on the flow background that can be calculated from the measured v_2^a and v_2^t , with only one common parameter ξ . The measured correlation function for 30-40% centrality bin is shown Fig.4. Several interesting features can be readily identified. First going from in plane to out of plane direction, the effective $v_{2,\text{eff}}^t$ changes from positive to negative. All six correlation functions cross each other at $\pm\pi/4$ and $\pi \pm \pi/4$, where the harmonic contribution is zero. The away side cross points are systematically higher than those at the near side, indicating that there is significantly more jet contribution at $\pi \pm \pi/4$ than at $\pm\pi/4$. The extremes of the

distributions are shifted to either the left or the right due to the jet contribution, so they does not peaks at $\pi/2$ where the flow contribution reaches maximum.

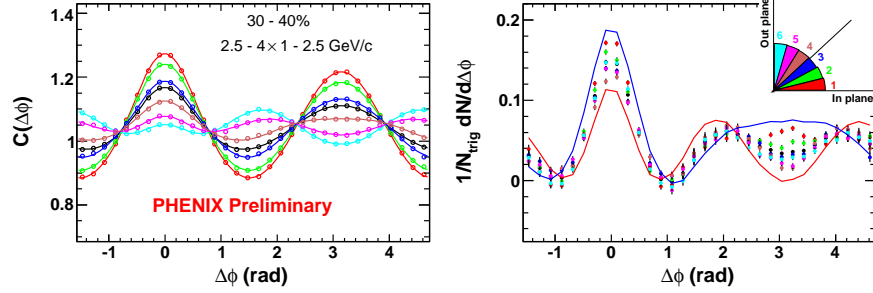


FIGURE 4. a) Correlation function for various 6 trigger direction bin and the trigger integrated bin (the center curve). b) The background subtracted per-trigger yields, the insert figure shows the 6 trigger bins.

By subtracting the flow contribution calculated according to Eq.2, we obtain the jet yield in each trigger direction as shown in Fig.4b. First we fix ξ using RP v_2 and ZYAM procedure without constraining the trigger direction. Then the flow term in each trigger bin can be calculated according to Eq.2 and thus fixed. Fig.5a shows the comparison of the the measured CFs and the calculated flow contributions. The systematic error bands correspond to the error of the RP v_2 , and are propagated using Eq.2. The size of the systematic error is largest for in plane bin and smallest for the out of plane bin. Thus RP dependence helps us to constrain the v_2 systematics when its error is not dominated by the RP resolution.¹ Back to Fig.4b, jet yields for different trigger

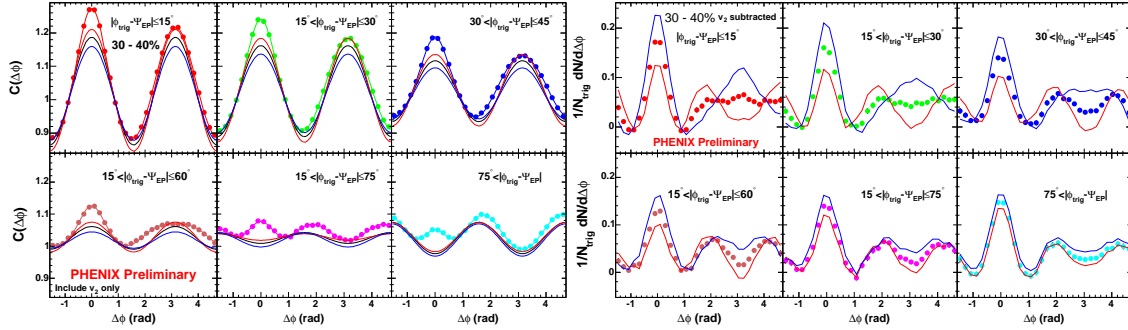


FIGURE 5. a) Correlation function and b) background subtracted per-trigger yield for the 6 trigger direction bins.

bins fall within the error band calculated for all six bins combined, however the shapes of the data have some differences. We believe the differences are mostly due to the remaining v_2 and the small v_4 contributions which we haven't take into account so far. In Fig.6, the difference of the per-trigger yield between in plane direction and out of plane direction: $(1/N_{\text{trig}} \Delta N / \Delta \phi)_{\text{in}} - (1/N_{\text{trig}} \Delta N / \Delta \phi)_{\text{out}}$ is plotted, and they are fitted with $c_0 + c_2 \cos 2\Delta\phi + c_4 \cos 4\Delta\phi$ term. Indeed most of the variations can be accounted for by this function. There is a small excess on the away side relative the near side in

¹ Since $v_2^a = v_{2,\text{raw}}^a / \langle \cos 2\Psi \rangle$, the error of v_2 due to RP resolution ($\langle \cos 2\Psi \rangle$) is independent of trigger direction.

30-40% centrality bin. This excess could be the hint for the path length dependence of the away side jet modification.

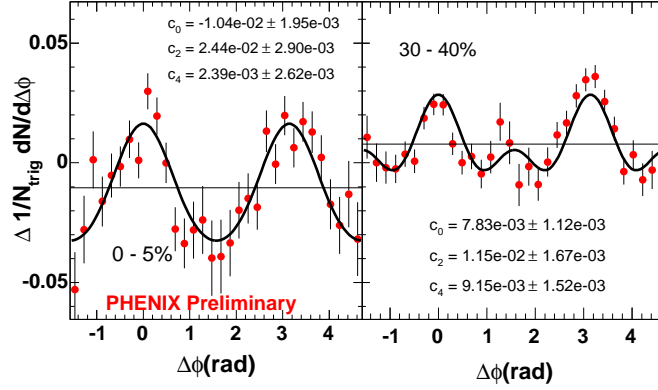


FIGURE 6. Difference of the in plane and out of plane per-trigger yield for a) 0-5% and b) 30-40% centrality bins.

REAPPEARANCE OF THE AWAY SIDE JETS.

With the significantly improved Au + Au statistics, it become possible to study the jet correlation at higher p_T . The importance of high p_T correlation is two fold. On the one hand, high p_T are dominantly coming hard process and are free from complicated intermediate p_T physics (for example recombination), thus can serve as a cleaner probe of the medium. On the other hand, knowledge on the properties of these high p_T jets can be used to disentangle normal jet fragmentation from other complicated medium contributions such as cherenkov gluons, shock wave and fragmentation of radiated gluons which become dominating at intermediate or low p_T .

To begin with, we present in Fig.7 several CFs in successively higher p_T ranges in central Au + Au collisions. The typical away side cone structure persists to $p_T \approx 4$ GeV/c, but the edges of the cones become sharper and their magnitude drops. In $4 - 5 \times 4 - 5$ GeV/c bin, away side jet is consistent with flat with fairly large statistical fluctuation. This could still be consistent with the cone structure, but it's magnitude must be significantly reduced.

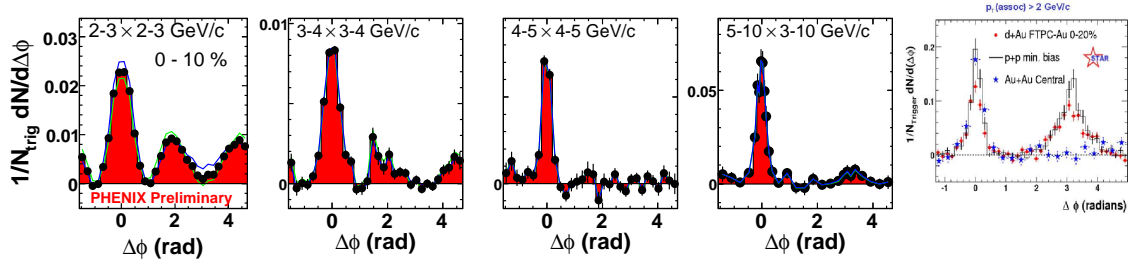


FIGURE 7. (left four panels) : per-trigger yield for different p_T selection in 0-10% centrality bin. (right panel): per-trigger yield from STAR in 0-10% centrality bin.

As a comparison, in the most right panel of Fig. 7, we also show the hadron-hadron correlation in Au + Au collisions from STAR. The data are for 0-10% most central Au

+ Au with $4 < p_{T,\text{trig}} < 6$ GeV/c and $2 < p_{T,\text{assoc}} < p_{T,\text{trig}}$, so they are comparable to the middle panel in Fig. 7. It is also almost comparable to the highest p_T point in Fig. 3a, where the p_T selection of the trigger and associated hadrons are swapped.² All three are qualitatively similar to each other. Interestingly, STAR's data are consistent with zero around π , but it seems to have a shoulder at $\pi \pm 1$. So maybe the “disappearance of away side jet” simply reflect a large suppression at $\Delta\phi \approx 0$, the small shoulder contribution is still visible as suggested by the right panel of Fig. 7.

In the highest p_T bin of Fig.7, a peak structure seems to reemerge around π on top of a pretty flat background. To understand the physics behind the peak structure, we plot in Fig.8 the centrality dependence of the CF for $5 - 10 \times 3 - 10$ GeV/c selection. It seems that the away peak structures exist in all centrality bins, although the magnitudes of the peaks are suppressed toward central collisions. At this point, it is hard to say whether the widths of the away peaks are also broadened in central collisions. On the other hand, there seems to be little change in both the shape and magnitude of the near side jet as function of centrality. During quark matter 2005, STAR's has shown di-jet correlation at much larger p_T ($8 < p_{T,\text{trig}} < 15$ GeV/c and $6 < p_{T,\text{assoc}}$ GeV/c) [17]. They find that for away side jet pairs at fairly large z ($z > 0.4 - 0.5$), the jet width and the shape of the fragmentation function are independent of p_T . In energy loss picture, the large z requirement bias the detected away side jets to small energy loss. Small energy loss requirement bias the detected jet towards surface, thus points to the picture where both jets are emitted tangential to the surface. If this scenario is true, we should recover the strong modification at low z (by decreasing $p_{T,\text{assoc}}$). To check this, in Fig.9a we shows the CF for various associated hadron p_T with trigger p_T fixed. The $\langle z \rangle$ of the associated hadron in the four panels are approximately 0.2, 0.4, 0.6 and 1. Clearly we see a stronger distortion of the away side jet shape at smaller $p_{T,\text{assoc}}$, the yields relative to the near side are also larger at smaller $p_{T,\text{assoc}}$. This is consistent with picture where a large fraction of low p_T associated hadrons comes from the processes initiated by the away side parton, such as shock wave or radiated gluons. In fact, the fragmentation function from STAR indeed suggest a significant deviation from the uniform scaling shape at $z \lesssim 0.4$ as shown in Fig.9b. So it is very important to measure the fragmentation function in full z range in order to constrain the bias effect.

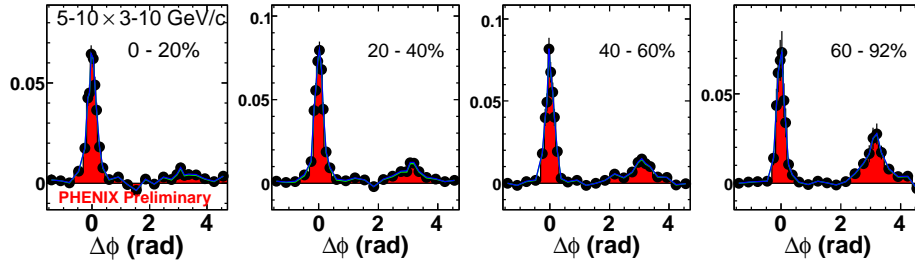


FIGURE 8. Centrality dependence of the per-trigger yield at high p_T

² When the p_T range of trigger and associated particle are swapped, the di-jet modification factor I_{AA} are connected to each other by, $I_{AA}^1/I_{AA}^2 = R_{AA}^2/R_{AA}^1$, where R_{AA}^1 and R_{AA}^2 are the nuclear modification factor of the first and second particle, respectively.

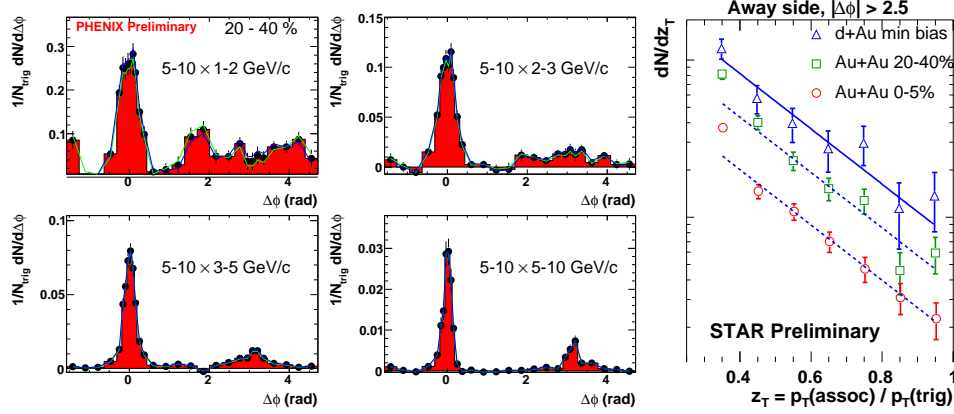


FIGURE 9. (left four panels): per-trigger yield for different $p_{T,\text{assoc}}$ in 20-40% centrality bin when trigger p_T is fixed. (right panel) Away side jet fragmentation from STAR [17].

CONCLUSIONS

In summary, jet properties from hadron-hadron correlation have been studied as function of p_T , centrality and the angle relative to the reaction plane. Precise extraction of jet signal relies on experimental control on the flow background, which can be constrained by looking their reaction plane dependence. Jet shape and yield are found to be strongly modified at intermediate and low p_T . The interpretations of these modification, however, are complicated by various competing mechanisms. By increasing the p_T for both triggering and associated hadrons, away side jet peak reappears but it's yield is suppressed. This could be result of the bias effect where the detected di-jets are emitted tangential to the surface.

REFERENCES

1. K. Adcox *et al.* [PHENIX Collaboration], Nucl. Phys. A **757** (2005) 184; J. Adams *et al.* [STAR Collaboration], Nucl. Phys. A **757** (2005) 102; B. B. Back *et al.* [PHOBOS Collaboration], Nucl. Phys. A **757** (2005) 28; I. Arsene *et al.* [BRAHMS Collaboration], Nucl. Phys. A **757** (2005) 1.
2. C. Adler *et al.* [STAR Collaboration], Phys. Rev. Lett. **90**, 082302 (2003)
3. J. Adams *et al.* [STAR Collaboration], arXiv:nucl-ex/0501016.
4. S. S. Adler *et al.* [PHENIX Collaboration], arXiv:nucl-ex/0507004.
5. J. Jia, J. Phys. G **31**, S521 (2005) [arXiv:nucl-ex/0409024].
6. N. N. Ajitanand *et al.*, Phys. Rev. C **72**, 011902 (2005)
7. Nathan Grau [PHENIX Collaboration], quark matter proceedings.
8. I. Vitev, arXiv:hep-ph/0506281.
9. I. M. Dremin, JETP Lett. **30** (1979) 140 [Pisma Zh. Eksp. Teor. Fiz. **30** (1979) 152].
10. V. Koch, A. Majumder and X. N. Wang, arXiv:nucl-th/0507063.
11. N. Armesto, C. A. Salgado and U. A. Wiedemann, arXiv:hep-ph/0411341.
12. J. Casalderrey-Solana, E. V. Shuryak and D. Teaney, arXiv:hep-ph/0411315.
13. J. Bielcikova, S. Esumi, K. Filimonov, S. Voloshin and J. P. Wurm, Phys. Rev. C **69**, 021901 (2004)
14. A. Drees, H. Feng and J. Jia, Phys. Rev. C **71** (2005) 034909
15. S. S. Adler *et al.* [PHENIX Collaboration], Phys. Rev. Lett. **91** (2003) 172301
16. S. S. Adler *et al.* [PHENIX Collaboration], Phys. Rev. C **71** (2005) 051902
17. Dan magestro [STAR Collaboration], arXiv:nucl-ex/0510002.